

Antiferromagnetic Ordering on CoO(001) Studied by Metastable Helium Beam Diffraction

P. Banerjee, X. Liu, M. Farzaneh, C.R. Willis, W. Franzen, and M. El-Batanouny
Department of Physics, Boston University, 590 Commonwealth Avenue, Boston MA 02215

V. Staemmler

Lehrstuhl für Theoretische Chemie, Ruhr-Universität Bochum, Germany

Magnetic diffractive scattering of coherent metastable helium atomic beams from CoO(001) surfaces reveal the presence of an anomalous enhancement in the intensity of the half-order antiferromagnetic diffraction peak over the temperature range of 250-320K. Electronic cluster calculations based on Hartree-Fock states with configuration interactions, together with mean-field and Monte Carlo studies of this system suggest that this behavior is associated with low-lying surface spin excited states.

PACS numbers: 68.35.Rh, 68.49.Bc, 75.10.Dg, 75.25.+z, 75.70.Rf, 75.80.+q

The magnetic properties of surfaces and thin films are currently a topic of much interest. This arises from the fact that these properties may be completely different from their bulk counterparts. For example, a pure surface magnetic ordering transition can occur at a temperature T_c^s higher than the bulk transition temperature T_c^b . A possible occurrence of such a phenomenon in gadolinium and terbium has been the subject of several papers[1, 2, 3]. More recently, our group reported on the critical behavior of antiferromagnetic (AFM) ordering on the NiO(001) surface[4], as measured by metastable He beam (He^*) diffraction. These measurements have shown a surface Néel temperature higher than the bulk value. Further, the temperature dependence of the sublattice magnetization showed a cross-over behavior consistent with the *extraordinary surface transition* belonging to the universality class of the semi-infinite anisotropic Heisenberg model[5].

In this Letter, we show that the AFM ordering on the CoO(001) surface, as measured by He^* diffraction, exhibits an anomalous enhancement over the temperature range between 250 K and 320 K, straddling the bulk Néel temperature T_N^b of 290 K. At T_N^b , the enhancement is suppressed and a dip in the magnetic diffraction peak intensity is observed.

CoO belongs to the family of AFM 3d transition-metal monoxides with a rocksalt structure in the paramagnetic phase. The spin-ordering in the bulk is characterized by ferromagnetic (111) spin sheets that are stacked antiferromagnetically[6]. On the (001) surface, this arrangement leads to a (2×1) AFM spin structure. Our experimental He^* diffraction measurements, shown in Fig. 1, display half-order magnetic peaks along the $\langle 10 \rangle$ and $\langle 01 \rangle$ directions, and no $(\frac{1}{2}, \frac{1}{2})$ peak along the $\langle 11 \rangle$ direction, not shown, and support the existence of such an AFM structure on the CoO(001) surface.

It has been established [7, 8] that the lowest bulk crystal-field (CF) split orbital state, ${}^4\Gamma_4$ (${}^4T_{1g}$), has an effective angular momentum $l = 1$ and is twelve-fold de-

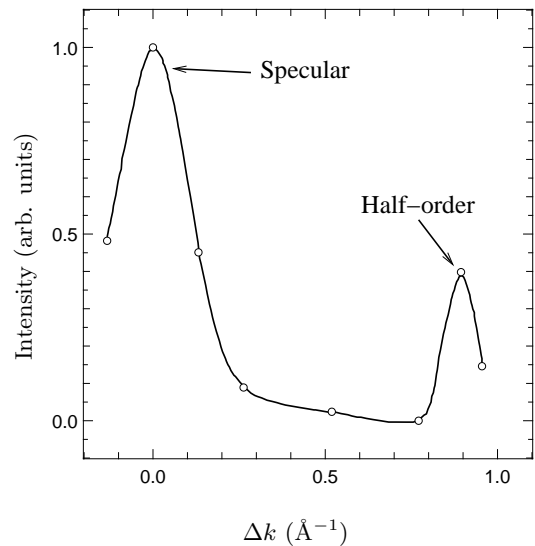


FIG. 1: Diffraction spectra measured along the $\langle 01 \rangle$ direction on CoO(001).

generate. This degeneracy gives rise to a strong Jahn-Teller instability, which is stabilized via spin-orbit (SO) interactions, giving rise to a $j = 1/2$ ground-state (GS), and $j = 3/2, 5/2$ excited-state (ES) manifolds. In the GS, a hole occupies a $Y_2^{\pm 1}$ -type orbital, which reduces the repulsion between a Co^{2+} ion and its neighboring O^{2-} ion. This leads to an appreciable tetragonal contraction of $\sim 1.2\%$ (at low temperatures) along one of the principal crystallographic axes[8]; about two orders of magnitude greater than the magnetostriction observed in the other monoxides[9]. Recently we have carried out electronic cluster calculations employing Hartree-Fock states with configuration interactions for bulk CoO which confirm all the above features. A detailed description of the methodology and results are given in Ref. [10].

In earlier publications[4, 11, 12, 13, 14] we demonstrated that He^* diffraction is very sensitive to surface

AFM ordering. In particular, in Ref. [4] we have shown that the microscopic origin of He* magnetic scattering can be accounted for by an imaginary, spin-dependent component of the He*- surface interaction potential of the form $\Delta V^S(\mathbf{r}) \propto i \mathcal{D}[S(\mathbf{R}); z] \langle S_z(\mathbf{R}, T) \rangle$, where $\langle S_z(\mathbf{R}, T) \rangle$ is the thermally-averaged z -component of the spin at (\mathbf{R}, z) and $\mathcal{D}[S(\mathbf{R}); z]$ is the corresponding local surface density of states. Within the framework of the eikonal approximation, the diffractive scattering amplitude $\tilde{\mathcal{A}}_{\mathbf{G}}$, resulting from the above imaginary potential, together with a corrugated hard-wall real component of the surface potential, with a corrugation shape function $\zeta(\mathbf{R})$, is given by

$$\tilde{\mathcal{A}}_{\mathbf{G}} = \frac{e^{-(W+\alpha)}}{\Omega} \int_{u.c.} d\mathbf{R} \exp \{ i[\mathbf{G} \cdot \mathbf{R} + q_z \zeta(\mathbf{R}) - \xi(\mathbf{R}) \langle \hat{S}_z(\mathbf{R}) \rangle] \} \quad (1)$$

where Ω is the area of the surface primitive mesh, W is the Debye-Waller factor and α is an attenuation factor accounting for He* beam decay through the Penning ionization channel. $\xi(\mathbf{R})$ includes $\mathcal{D}[S(\mathbf{R}); z]$ plus other constants. In the case of the (2×1) spin-ordering, the diffraction amplitude of the $\frac{1}{2}$ -order peak is related to the average sublattice magnetization by [4]

$$\mathcal{A}_{(1/2,0)} = e^{-(W+\alpha)} I_1(x), \quad (2)$$

where $x \propto \langle \hat{S}_z(\mathbf{R}) \rangle$ and $I_1(x)$ is a modified Bessel function of order one.

The details of the design and operation of our experimental facility have been presented earlier in Ref. [4]. Beam intensities of about 3×10^5 He* atoms s^{-1} at the sample surface were achieved in the present measurements. All of the data were obtained from CoO(001) surfaces freshly cleaved in vacuum, with a background pressure less than 10^{-10} Torr with He beam turned off. The CoO sample rods were attached to a copper sample holder with silver conducting epoxy. A silicon diode was attached at the base of the sample holder to measure and control the sample temperature. The temperature controller (Scientific Instruments Inc. Model 9600-1) is factory calibrated and is accurate to ± 0.5 K. Scans were taken at 2 K increments between 250 K and 320 K and at larger increments at lower temperatures. Measurements of the diffraction intensities consistently yielded a minimum in the $\frac{1}{2}$ -order magnetic diffraction peak intensity at $T_N^b \simeq 290$ K for all cleaved surfaces, irrespective of their distance from the silicon diode. We determined T_N^b to be 290 ± 0.2 K by measuring the specific heat of several bulk samples as a function of temperature with a Perkin-Elmer model DSC7 differential scanning calorimeter.

Fig. 2 represents data collected from a single cleave and displays the enhancement of the peak intensity both below and above T_N^b . Fig. 3 depicts data collected from several cleaves and shows more details of the enhancement

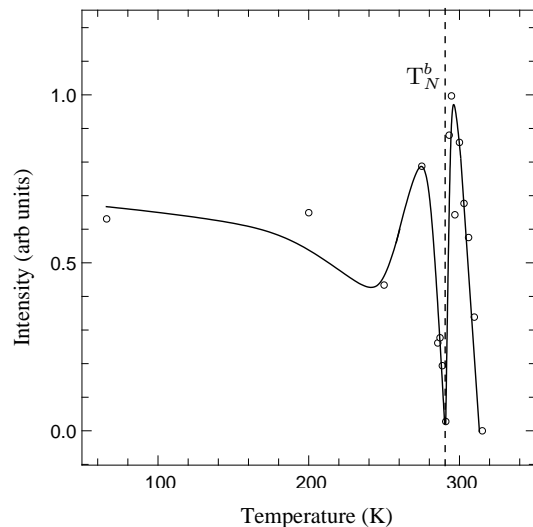


FIG. 2: Half-order peak intensity as a function of surface temperature. Data shown is from a single cleaved surface. The dashed line demarks the bulk Néel temperature. The solid line is a guide to the eye.

below T_N^b . We notice that the peak intensity decreases slightly with increasing temperature from 50 K to about 250 K, but then exhibits an anomalous increase with further increase in temperature, reaching a maximum at about 280 K, followed by a steep decrease, reaching a minimum at T_N^b . Above T_N^b it increases once more to a maximum at 310 K and finally disappears at about 320 K. This behavior has been checked repeatedly and was always reproducible even for different crystal ingots.

To investigate these anomalous effects, first, we extended our electronic cluster calculations to the CoO(001) surface. Under the C_{4v} symmetry of the surface, the 4T_4 state splits into a nondegenerate A_2 and doubly-degenerate E orbitals, separated by 50 meV, comparable to SO interaction energies, so that the latter cannot be treated as a perturbation on the CF state. A balanced calculation shows that all the ensuing states are Kramers doublets. The first ES doublets lie at 29 and 94 meV above the GS. We also find that the expectation value of the spin in the GS and first ES to be $\langle s_z \rangle \simeq 1/2$ and $\langle s_z \rangle \simeq 3/2$, with z normal to the surface.[10]

Next, we constructed a model Hamiltonian that describes the low-lying spin states and includes magnetoelastic effects. We started with the SO eigenstates of the Co^{+2} as a basis set and focused on the lowest-lying manifold ${}^4F_{3/2}$. By using the operator-equivalent formalism (OEF)[15], a spin representation for the surface CF Hamiltonian is obtained as $\mathcal{H}_{CF} = cS_z^2$. \mathcal{H}_{CF} splits the ${}^4F_{3/2}$ manifold into two doublets: $m_s = \pm 3/2$ and $m_s = \pm 1/2$ with an energy gap of $\Delta_0 = 2c = 29$ meV. We added the effect of the tetragonal lattice distortion on the crystal field, by introducing a uniform sur-

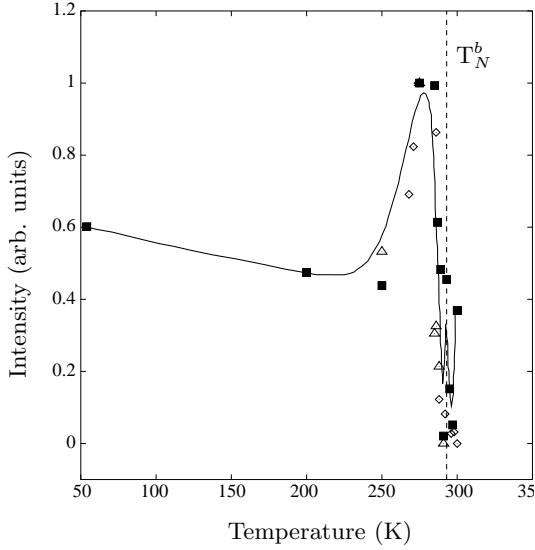


FIG. 3: Intensity of the magnetic half-order diffraction peak as a function of surface temperature. Data shown is collected from several different cleaved surfaces, as indicated by solid and open circles and triangles. The dashed line demarks the bulk Néel temperature. The solid line is a guide to the eye.

face tetragonal strain field η , which, in the OEF, has the form $b\eta S_z^2$, where b is the magnetoelastic constant, and modifies \mathcal{H}_{CF} as $\mathcal{H}_{CF} = (\frac{\Delta_0}{2} + b\eta) S_z^2$. The model Hamiltonian can then be written as

$$\mathcal{H} = \sum_{\alpha} \mathcal{H}_{CF}^{\alpha} + \sum_{\beta} \mathcal{H}_{CF}^{\beta} + J_2 \sum_{\langle nnn \rangle_{\alpha\beta}} \mathbf{S}_{\alpha} \cdot \mathbf{S}_{\beta} + \frac{\kappa}{2} \eta^2 + \sigma \eta, \quad (3)$$

where α, β denote the two AFM sublattices and σ represents a uniform bulk tetragonal stress field that couples to the surface strain; it has the experimentally measured temperature-dependent form [16, 17] $\sigma = \sigma_0 \left(1 - \frac{T}{T_N^b}\right)^{0.6}$. We evaluated the free energy of the system using the Bogoliubov-Peierls mean field variational method[18] with a trial noninteracting Hamiltonian of the form

$$\mathcal{H}_0 = \sum_{\alpha} \left(\mathcal{H}_{CF}^{\alpha} - h_{\alpha} S_{\alpha}^z \right) + \sum_{\beta} \left(\mathcal{H}_{CF}^{\beta} - h_{\beta} S_{\beta}^z \right) + \frac{\kappa}{2} \eta^2 + \sigma \eta, \quad (4)$$

where $h_{\alpha, \beta}$ are the effective mean fields along the z -axis, taken as variational parameters. The temperature-dependence of the sublattice magnetization is then determined by solving the coupled self-consistent equations of the magnetization, $M(T)$:

$$M = \frac{1}{2} \frac{\sinh(2\beta J_2 M) + 3e^{-\beta \Delta} \sinh(6\beta J_2 M)}{\cosh(2\beta J_2 M) + e^{-\beta \Delta} \cosh(6\beta J_2 M)} \quad (5)$$

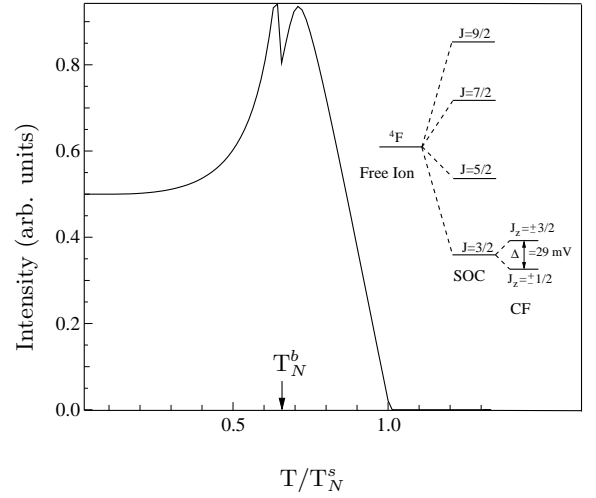


FIG. 4: Temperature-dependence of the half order peak intensity from a variational mean-field calculation.

and of the gap, $\Delta(T)$

$$\Delta = \Delta_0 - \frac{2\sigma b}{\kappa} - \frac{b^2 \cosh(2\beta J_2 M) + 9e^{-\beta \Delta} \cosh(6\beta J_2 M)}{2\kappa \cosh(2\beta J_2 M) + e^{-\beta \Delta} \cosh(6\beta J_2 M)}. \quad (6)$$

These equations are obtained by minimizing the free energy with respect to h_{α} , h_{β} and η . The solution of these equations is carried out using experimental values for σ and κ , as obtained from neutron scattering measurements[19] of the phonon spectra, which yields $\kappa = 600\Delta_0$.

The temperature-dependence of the half-order peak intensity $I_{(1/2,0)}(T)$ is determined by substituting the computed $M(T)$ into Eq. (2), with $W = 0$. Fig. 4 shows $I_{(1/2,0)}(T)$ where both the anomalous enhancement and the depression at T_N^b are manifested. It corresponds to $J_2/\Delta_0 = 0.25$ and $b = 8.8\Delta_0$, comparable to reported experimental values for CoO[20, 21].

A Monte-Carlo simulation, based on the following Hamiltonian

$$\begin{aligned} H &= H_s + H_{sb} + H_b \\ H_a &= J_a \sum_{\langle nnn \rangle} \vec{S}_i^a \cdot \vec{S}_j^a + \sum_i \left(\frac{\Delta_0^s}{2} + b_a \sum_k \eta_{i,k}^a \right) (S_{iz}^a)^2 \\ &\quad + \frac{\kappa_a}{2} \sum_i \sum_k (\eta_{i,k}^a)^2, \\ H_{sb} &= J_{sb} \sum_{\langle nnn \rangle} \vec{S}_i^s \cdot \vec{S}_j^b, \end{aligned} \quad (7)$$

also confirms the anomalous effects. Here, the indices s and b refer to surface and bulk, respectively, and

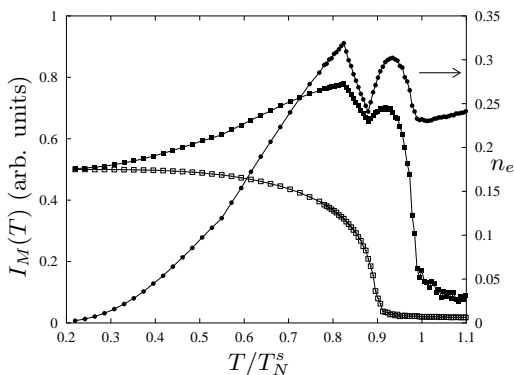


FIG. 5: Computed surface magnetization (filled squares), bulk magnetization (open squares) and the excited state population (filled circles) as a function of temperature.

$a = s$ or b . The sum over k runs over all the nearest-neighbor O^{-2} ions for a Co^{+2} ion at site i . We show typical results in Fig. 5 for a $20 \times 20 \times 33$ slab with periodic boundary conditions. Filled squares represent the magnetic diffraction peak intensities for the surface, $I_M^s(T)$ with the Debye-Waller factor $W = 0$, while the open squares show the corresponding intensities for the bulk, $I_M^b(T)$. $I_M^s(T)$ manifests both the anomalous enhancement and the dip at T_N^b , similar to both experimental and mean field results. It also shows that $T_N^s > T_N^b$.

The filled circles in Fig. 5 depict the population of the excited state n_e , which mimics the behavior of $I_M^s(T)$ in the anomalous region. n_e is appreciably higher than would be expected from thermal activation across the gap Δ_0 . We also note that the bulk spins do not populate the $j = 3/2$ manifold, since the energy gap is much higher than T_N^b .

Despite the fact that both mean field and Monte-Carlo results show a suppression in the intensity at T_N^b , a much more pronounced attenuation is observed in the experiment. This difference in the magnitude of attenuation can be attributed to the fact that the model we used is a simple one with the simplest choice for crystal field potential and magnetoelastic coupling. But it should be emphasized that even with the current model, the most important features of the experimental results, namely the enhancement and the suppression of the intensity at T_N^b are captured.

In conclusion, the following picture emerges from the results presented above. At low enough temperatures, the ordered AFM bulk spins pin the surface spins to the

$s_z = 1/2$ state. As the temperature increases, the bulk spin ordering decreases and the surface spins, less constrained by the bulk, re-orient by populating the first $s_z = 3/2$ excited state. The reorientation arises because of two contributions to the free energy: The energy of the $3/2$ -state is lowered by an amount $\sim S^2 J_s$ through coupling to surface neighbors, with $S = \pm \frac{3}{2}$, and the entropy is increased by populating new states. The depression in half-order peak intensity at T_N^b is due to magnetoelastic coupling to the bulk.

This work is supported by the U.S. Department of Energy under Grant No. DE-FG02-85ER45222.

-
- [1] D. Weller *et al.*, Phys. Rev. Lett. **54**, 1555 (1985).
 - [2] H. Tang *et al.*, Phys. Rev. Lett. **71**, 444 (1993).
 - [3] C. Rau, C. Jin, and M. Robert, J. Appl. Phys. **63**, 3667 (1988).
 - [4] M. Marynowski, W. Franzen, M. El-Batanouny, and V. Staemmler, Phys. Rev. B. **60**, 6053 (1999), and references therein.
 - [5] H. Diehl and E. Eisenriegler, Phys. Rev. B. **30**, 300 (1984).
 - [6] W. Roth, Phys. Rev. **110**, 1333 (1958).
 - [7] C. Wang, K. Fink, and V. Staemmler, Chem. Phys. **192**, 25 (1995).
 - [8] J. Kanamori, Prog. Theor. Phys. **17**, 177 (1957).
 - [9] T. G. Phillips and R. L. White, Phys. Rev. **153**, 616 (1967).
 - [10] V. Staemmler and K. Fink, Chem. Phys. **278(2-3)**, 79 (2002).
 - [11] A. Swan *et al.*, Phys. Rev. Lett. **71**, 1250 (1993).
 - [12] A. Swan *et al.*, J. Vac. Sci. Technol. A **12**, 2219 (1994).
 - [13] M. Marynowski *et al.*, Surfaces and Interface Analysis **23**, 105 (1995).
 - [14] M. El-Batanouny, J. Phys.: Condens. Matter **14**, 6281 (2002).
 - [15] B. Bleaney and K. Stevens, Rep. Prog. Phys. **16**, 108 (1953).
 - [16] W. Jauch, H. Bleif, and F. Kubanek, Phys. Rev. B **64**, 052102 (2001).
 - [17] M. Rehtin and B. Averbach, Phys. Rev. Lett. **26**, 1483 (1971).
 - [18] R. Feynman, in *Statistical Mechanics* (Addison Wesley, 1998).
 - [19] J. Sakurai, W. Buyers, R. Cowley, and G. Dolling, Phys. Rev. **167**, 510 (1968).
 - [20] J. Kanamori, Prog. Theor. Phys. **17**, 197 (1957).
 - [21] D. Herrmann-Ronzaud, P. Burlet, and J. Rossat-Mignod, J. Phys. C:Solid State Phys. **11**, 2123 (1978).